https://dx.doi.org/10.1016/j.cemconcomp.2019.103425

Investigation on expansion effect of the expansive agents in ultra-high performance concrete

Peiliang Shen[1,2] , Linnu Lu[1,b], Yongjia He[1], Fazhou Wang[1,a], JianXin Lu[2], Haibing Zheng[2],Shuguang Hu[1]

([1] State Key Laboratory of Silicate Materials for Architectures, Wuhan University of Technology, Luoshi Road 122, Wuhan, 430070, China)

([2]Department of Civil and Environmental Engineering, The Hong Kong Polytechnic University, Hung Hom, Kowloon, Hong Kong)

[a] Corresponding author, E-mail: fzhwang@whut.edu.cn

[b] Corresponding author, E-mail: 383337652@qq.com

Abstract: In this study, the expansion mechanisms of calcium-sulfoaluminates -CaO based expansive agent (CSA-CaO EA) on the volume stability of ultra-high performance concrete (UHPC) were systematically studied. The test results show that the incorporation of CSA-CaO EA is beneficial to reduce the autogenous shrinkage of UHPC effectively due to the formation of additional $Ca(OH)_2$ and ettringite. However, the reduction of early autogenous shrinkage is limited and the cracking risk is still very high when the addition of CSA-CaO EA reaches 15% of binders. According to the results, the factors hindering the expansion effect of CSA-CaO EA include the low w/b ratio, compact microstructure, out-sync of time "window" of expansion and shrinkage and the potential exchange of water between solids. Strategies and experimental validations on improving the shrinkage compensation are discussed. It indicates that the expansive UHPC can be prepared by using an CaO based EA with high reactivity and low water consumption via controlling the time "window" of expansion.

Keywords: Ultra-high performance concrete; autogenous shrinkage; expansive agent; hydration; expansion

1 Introduction

UHPC is a kind of advanced cement based material developed by François in 1990s[1], which exhibits ultra-high mechanical properties and excellent durability. These ultra-high performances are attributed to the optimization of particle size of each component in the mixture based on packing theory and low water to binder (w/b) ratio[2, 3]. However, the high volume fraction of superfine particles, free of coarse aggregate and low w/b ratio would lead to the occurrence of high autogenous shrinkage at an early age[4]. The high shrinkage may induce cracks and further impair the durability of UHPC[5, 6]. Therefore, it is of great significance to find solutions to reduce the shrinkage for the potential application of UHPC.

The autogenous shrinkage and dry shrinkage, which occur after final setting of concrete, have been widely investigated in the past few decades, and the sum of these two kinds of shrinkage are taken as the total shrinkage. Moreover, the autogenous shrinkage is caused by the withdrawal of water from capillary pores due to hydration, and eventually becomes the dominant role of total shrinkage in concrete with low w/b ratio [7-9]. In order to reduce the autogenous shrinkage, many approaches have been developed[10, 11]. Among, there are mainly three kinds of strategies: (a) decrease the surface tension of pore solution by adding shrinkage reducing admixtures[12], (b) internal curing by adding lightweight aggregate [13, 14], super absorbent polymer [15-17] and rice husk ash [18, 19] etc., (c) compensate shrinkage by adding expansive agent (EA)[20, 21]. The compensation of shrinkage by adding EA is one of the effective methods, which was widely used for the crack prevention[22]. The mostly common method for reducing shrinkage and producing expansive concrete is to form expansive ettringite [11], other EAs such as free lime-based EA and MgO-type EA are also used[23-25]. Among different ettringite-triggered EAs, the CSA based EA is the most commonly used[26, 27].

For UHPC with very low w/b ratio, the ettringite based EA has been applied to reduce the autogenous shrinkage and dry shrinkage of UHPC[26-28]. According to Park's work, the 28 d-free shrinkage strain of UHPC with 7.5% EA was reduced by 44% compared to the reference specimen[3]. The reduction of shrinkage was due to the formation of ettringite[29]. Generally, different ettringite based EA could reduce the autogenous shrinkage of UHPC obviously[3, 29-31]. However, the formation of ettringite requires a large amount of free water [32], but the water is not enough in UHPC itself due to the very low w/b ratio[33]. This would restrain the expansion effect

of the EA and result in a less effective in the shrinkage reduction of UHPC. Therefore, the UHPC containing conventional ettringite based EA still showed relatively high autogenous shrinkage[34-36].

Meanwhile, most of these previous studies focused on the effect of EA on the autogenous shrinkage and mechanical properties. Limited information on the expansion mechanism of EA in UHPC was reported. The expansion mechanism of ettringite based EA in UHPC was still not clear. In order to make the EA more effective in reducing the shrinkage and restraining shrinkage cracking of UHPC, a combination of CSA and CaO was adopted as EA in UHPC. The expansion mechanism of the EA in UHPC was systematically studied in this study and the critical factors controlling the expansion property of EA in UHPC was analyzed. Based on the mechanism, remarks and applications in promoting expansion effect of EA in UHPC can be conducted, aiming at achieving low shrinkage and even expansion.

The objective of this research is to investigate the effects of CSA-CaO EA on the performance of UHPC and expansion mechanism of CSA-CaO EA in UHPC, aiming at finding approaches to improve the expansion effect of expansive agent and preparing a low-shrinkage or expansive UHPC. The mechanical properties, autogenous shrinkage and internal relative humidity (RH) of UHPC were determined. Other techniques including the scanning electron microscopy (SEM), X-ray diffraction (XRD), isothermal calorimetry and thermal analysis were applied to characterize the effect of CSA-CaO EA on the microstructure and hydrates of UHPC. The effect of w/b ratio on the pore structure and relative humidity were studied to discover the critical factors controlling the expansion property of CSA-CaO EA. Based on expansion mechanisms of CSA-CaO EA in UHPC, strategies for improving the expansion efficiency of EA in UHPC were proposed.

2 Materials and methods

2.1 Materials and mixture proportions

Portland cement produced by Huaxin cement Co. Ltd. was used to prepare the UHPC specimens. The silica fume and fly ash used were produced by WISCO group. The CSA-CaO based EA sourced from Tianjin Baoming Co. Ltd was selected to study its expansion effect in UHPC. The main expansive minerals are CaO and CSA, and the weight ratios of CSA and CaO in CSA-CaO EA are 46.2% and 22.7%, respectively. The 7d-restrained expansion rate in water of CSA-CaO

based EA is 0.06% (tested according to Chinese standard GB 23439-2009 [37]). The high reactive CaO based EA produced by Wuhan Sanyuan special building material Co., Ltd. was also used, which was grinded to a Blaine fineness of 612.3 m^2/kg. The weight ratios of CaO and sulfo-aluminate in CaO based EA are 70.21% and 7.93%, respectively. The 3d-restrained expansion rate in water of CaO based EA is 0.12% and the 7d-restrained expansion rate is 0.14%. The oxide compositions of the Portland cement, silica fume, fly ash and EA tested by X Ray Fluorescence (model xios advanced) are listed in the Table 1. The Blaine fineness tested by the Blaine specific surface measure equipment (DBT-127) according to Chinese standard GB/T 8074-2008, specific gravity tested by Le Chatelier Flask according to Chinese standard GB/T 208-2014 and setting time determined by the Vicat apparatus according to Chinese standard GB/T 1346–2001 are listed in the Table 2. River sand with a diameter ranging from 0.15mm to 1.25mm was used as aggregate. A type of straight steel fiber (length=13mm, diameter=0.22mm) with tensile strength of 1100MPa is utilized. A high effective polycarboxylate superplasticizer produced by Sobute New Materials Co,. Ltd was also used, and the water reducing rate is about 35%. Clean tap water was used for all mixtures.

Table 1 Oxide compositions of cementitious materials (wt. %)

Oxide	SiO_2	Al_2O_3	CaO	Fe_2O_3	SO_3	MgO	Na_2O	K_2O	LOI
Cement	21.70	4.76	63.01	3.57	2.81	1.61	0.13	0.59	1.82
Silica fume	88.29	0.14	0.92	0.19	1.51	3.21	0.14	0.17	5.26
CSA-CaO EA	5.90	26.62	37.44	2.07	19.20	2.01	0.56	0.30	5.34
Fly ash	49.20	37.93	3.01	3.62	0.65	0.35	0.34	0.85	4.05
CaO EA	4.28	5.55	73.81	0.89	6.68	1.32	0.43	0.23	5.83

Table 2 Physical properties of cementitious materials

Properties	Blaine fineness (m^2/kg)	Specific gravity	Setting time (min)	
			Initial	Final
Cement	351.7	3.10	230	295
Silica fume	15248.0	2.48	/	/
CSA-CaO EA	342.0	2.96	152	223
Fly ash	567.8	2.20	/	/
CaO EA	612.3	2.87	125	185

The mixture proportions of the UHPC were shown in Table 3. The UHPC pastes with the same w/b to that of UHPC were prepared for microstructure analysis. The UHPC specimens with the w/b ratios of 0.25, 0.3 and 0.4 were also prepared for internal RH test. The mixing and casting procedures were adjusted to obtain advanced properties of UHPC, which was shown as follows: (1)

All the powders were added into a mixer and mixed for one minute; (2) then, the superplasticizer and water were added into the mixer and mixed for three minutes; (3) Afterwards, the sand and steel fiber were added and mixed for two minutes mixing at low speed and then mixed for another two minutes at high speed. The workability of UHPC was tested according to the Chinese standard (GB/T 2419-2005). The slump flow is shown in Table 3.

Table 3 Mixture proportions of the UHPC (kg/m^3) and the flow values

Name	Cement	EA	Silica fume	Fly ash	Sand	w/b*	superplasticizer	Steel fiber	Slump flow (mm)
UH1	720	0	160	80	1250	0.18	14.4	156	236.7
UH2	684	36 (CSA-CaO)	160	80	1250	0.18	14.4	156	235
UH3	648	72 (CSA-CaO)	160	80	1250	0.18	14.4	156	220
UH4	612	108(CSA-CaO)	160	80	1250	0.18	14.4	156	220
UH5	684	36(CaO)	160	80	1250	0.18	14.4	156	225
UH6	648	72(CaO)	160	80	1250	0.18	14.4	156	203.3

* The binder consists of cement, silica fume, EA and fly ash

2.2 Methods

2.2.1 Autogenous shrinkage measurement

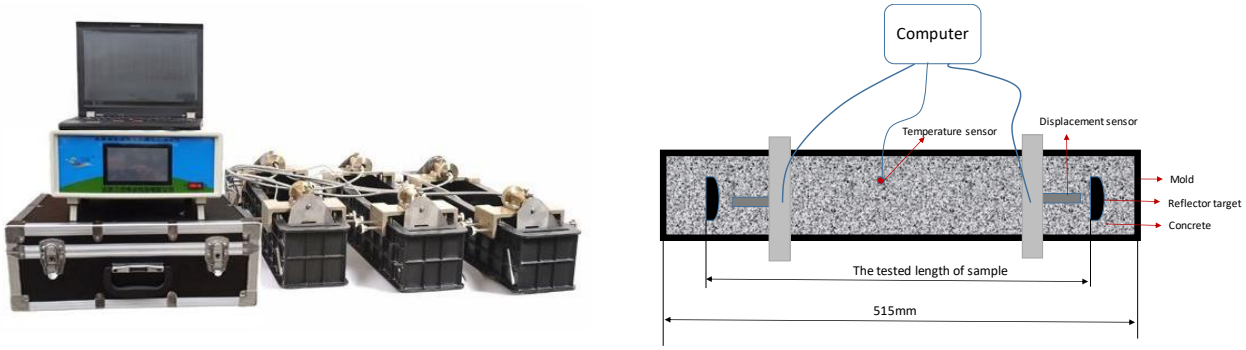

(a) The image of the device (b) The diagrammatic sketch of the device

Figure 1 Illustration of the device for autogenous shrinkage of UHPC measurement

The autogenous shrinkage was tested according to the Chinese standard GB/T 50082-2009. A non-contact deformation tester of concrete (model CABR-NES) was used accordingly. Figure 1 shows the test setup. Specimens with the size of 100mm ×100mm×515mm were stored in a climatic chamber with the temperature of 20℃±1℃ and relative humidity of 60±5%. The specimens were covered with polyethylene film during testing. The evolution of length of specimens were recorded every 1 minute at 15min later after mixing with water. In addition, the final setting time was tested by preparing another specimen with the same mixture proportion of specimens to examine the time for the start of autogenous shrinkage measurement. Three specimens for each batch were performed

to obtain an average value.

2.2.2 Mechanical properties

Specimens with a size of 40 mm×40 mm×160 mm were casted for mechanical properties measurement. The specimens were demolded at 24 h and were cured at the temperature of 20 ± 1℃ and relative humidity over 95%. The flexural strength and compressive strength of specimens were measured at the age of 3 d, 7 d and 28 d. The loading rate of compressive strength and flexural concrete were controlled at 2.4kN/s and 50N/s, respectively. A machine with maximum load of 300kN was used. The span for flexural strength test and the loading area for compressive strength were 100mm and 40×40mm^2, respectively. Three specimens were performed to further calculate the average strength.

2.2.3 X-ray diffraction analysis

A D8 Advance X-ray diffractometer from Bruker AXS employed with Cu Kα radiation (λ=1.5405Å) was used to conduct the X-ray diffraction analysis (performed at 35 kV and 30 mA). The 2-theta values range from 5° to 75°. The data was collected with a step size of 0.02° and a count time of 3 s per step. The search-match capabilities of XRD software JADE 7.0 (MDI, Livermore, CA, USA) and the patterns of the International Centre for Diffraction database were used to identify the phases in the samples. In order to quantify to amount of expansive product, UHPC paste were mixed with 20% corundum powders as internal standard substance. The measurement was conducted with the step size used was 0.020° and 0.5 seconds per step. Rietveld refinement quantitative analysis was conducted by using Topas 4.2 software. The UHPC pastes containing different additions of CSA-CaO EA were prepared and cured for 28d at the temperature of 20 ± 1℃ and relative humidity over 95%. Then, the hydration was stopped by soaking in ethanol. Before testing, the samples were dried at 45℃ in vacuum drying oven for 48h.

2.2.4 Scanning electron microscopy (SEM) test

A FEI QUANTA FEG 450 Environmental Scanning Electron Microscope equipped energy dispersive X-ray analysis system (FESEM, FEI, Hillsboro, OR, USA) was employed to study the morphology of UHPC with and without CSA-CaO EA. The microscope was operated at an accelerating voltage of 20kV, with a working distance of 12mm. Thin sections were made for SEM analysis. The UHPC specimens used for SEM analysis was cut into small fragments, and the

hydration of steam cured UHPC was stopped by soaking in ethanol. The thin Pt coating was applied by bombarding the metal with atoms of heavy gas and directing the atoms on the surface of specimens. Before the SEM testing, the specimens were dried at 45℃ in vacuum drying oven and stored in a drying vessel.

2.2.5 Heat of hydration and non-evaporable water content

A multi-channel isothermal calorimeter (model TAM Air, TA Instruments) was used to determine the normalized heat flow and cumulative heat of UHPC. The specimens without sand were prepared as the mixture proportions in Table 3. The measurement was carried out under an isothermal condition of 20℃±0.02℃. About 5g of dry cementitious materials was used for each specimen. The normalization basis of the measurement results is the total amount of cementitious material including the EA. The heat release was recorded continuously until 3d.

After curing for 1d, 3d, 7d and 28d, the hydration of UHPC was stopped by ethanol. The specimens were cut from the inner of test-piece and grinded into particles (<75μm). Before test, the specimens are grinded into powders and dried at 45℃ in vacuum drying oven for 48h to remove the ethanol. The specimens were firstly heated up to 105℃ until the mass is constant, and then the sample was transferred to a resistance furnace at 1050 ℃ for 3 h. Usually, the mass loss due to heating (between105℃ and 1050℃) is considered as non-evaporable water. In order to get rid of the influence of mass loss on ignition of other materials except non-evaporable water, the mass loss on ignition of raw materials would be considered when the non-evaporable water was measured.

2.2.6 Pore structure

The mercury intrusion porosimetry (MIP) was used to evaluate the effect of CSA-CaO EA and w/b ratio on the pore structure of UHPC. The AutoPore IV 9500 series pore size analyzer (Micromeritics Instrument Corporation) was used in this study. The mercury intrusion pressure between 0.00345 MPa and 413.7 MPa was employed for determining the pore structure. The equilibration time periods at low and high pressure stage are 20s and 30s respectively. The surface tension of mercury is 0.458N/m. The contact angle between the pore surface and mercury is set at 130°. The normal cement paste with of a w/b ratio of 0.4 and UHPC paste were prepared for MIP test at the age of 24h. The UHPC specimens with 10% CSA-CaO EA and without CSA-CaO EA were tested at 28d. The specimens were cut into pieces with particle size around 4mm-5mm. Before

testing, the hydration of UHPC was stopped by ethanol, and then the specimens were dried in vacuum drying oven at 60℃ for 48h.

2.2.7 Thermal analysis

A Power-Compensation Differential Scanning Calorimeter (model TGA STA449c/3/G) from NETZSCH Group was applied to conduct the thermal analysis. The thermal analysis was conducted at a heating rate of 10℃/min from 40℃ to 1000℃ under nitrogen atmosphere. The paste samples (without sand and steel fiber) with different CSA-CaO EA additions were prepared according to Table 3. The hydration of these samples was stopped by ethanol at the age of 1d, 3d, 7d and 28d. Around 10mg powders of each specimen was used for the measurement. Before test, the samples were grounded into powders with diameter smaller than 75μm and were dried under vacuum at 40℃.

2.2.8 Internal relative humidity

UHPC samples with a size of 100mm×100mm×100mm in dimension were used to test the internal relative humidity. A hole was prepared by adding a plastic sleeve at a depth of 50mm. A sensor was put in the center of the sample after molding to test the RH and temperature. The certainty of the measurement of RH and temperature are ±0.1%, and the test range of RH is between 0% and 100%. The testing interval is one second. The measurement was conducted at 1h after mixing. The samples were covered by polyethylene film to prevent possible water evaporation.

3 Results and interpretations

3.1 Effect of CSA-CaO EA on mechanical properties of UHPC

The compressive strength and flexural strength of UHPC containing different proportions of CSA-CaO EA (UH1 to UH4) are shown in Figure 2. It can be seen from these figures that the compressive strength and flexural strength of the reference sample reach 172.5 MPa and 39.9 MPa at 28d, respectively. The test results also show that the compressive strengths of UHPC with CSA-CaO EA are slightly higher than that of reference at the early age (at 3d), while the 7d and 28d-compressive strengths decrease when more than 5% CSA-CaO EA are added. The effect of CSA-CaO EA on flexural strength of UHPC shows a similar trend. The reduction in strength may be related to the possible micro-cracks resulting from expansion products and the loose of the

structure tissue with cracks due to the replacement of cement by CSA-CaO EA[38, 39]. This explanation is also supported by other previous studies, such as concrete containing CSA based expansive agent and CaO based expansive agent [8, 33, 40]. Therefore, proper amount of CSA-CaO EA should be considered to be introduced in UHPC as excess content of CSA-CaO EA will have an adverse effect on the mechanical properties.

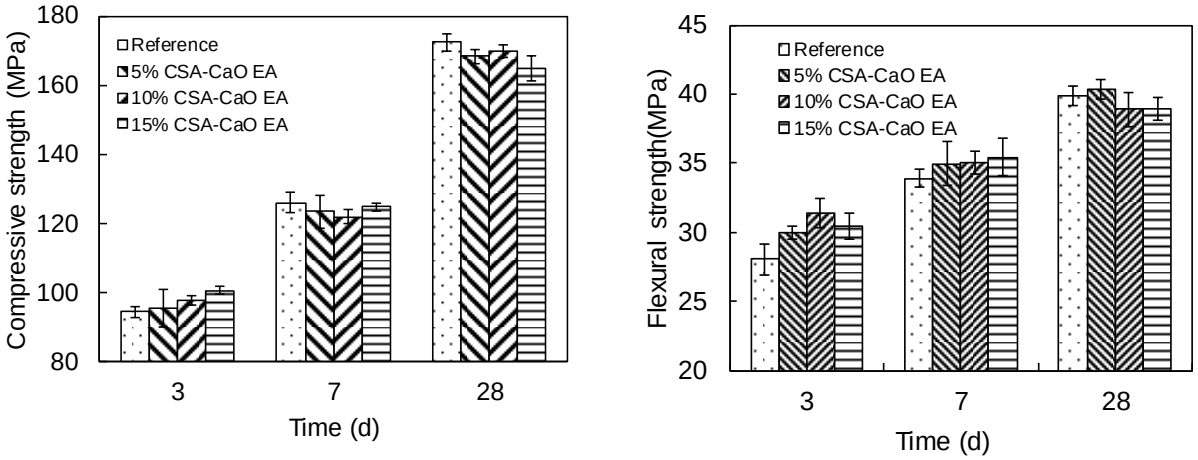

(a) The compressive strength (b) The flexural strength

Figure 2 The effect of CSA-CaO EA on mechanical properties of UHPC

3.2 Effect of CSA-CaO EA on autogenous shrinkage of UHPC

The Figure 3 shows the effect of CSA-CaO EA on the autogenous shrinkage development of UHPC without steel fibres. There is no doubt that the reference UHPC shows a significantly high shrinkage. The 7d-autogenou shrinkage is as high as 1700με. This is much higher than that of normal concrete with a high w/b ratio[41]. Based on the development of autogenous shrinkage, it can be divided into two stages. In the first stage (<24 h), the autogenous shrinkage develops rapidly. When the UHPC is setting, it starts to shrink and lead to high shrinkage value at 24 h. For the second stage, the autogenous shrinkage increases gradually after 24 h. Near 75% of 7d-shrinkage occurs before 24h. It can be concluded that the UHPC shows very high autogenous shrinkage at the early age, which will potentially induce crack and degrade its performance.

Additionally, the autogenous shrinkage decreases with the increasing CSA-CaO EA content, and the shrinkage curves are changed by adding CSA-CaO EA. Firstly, compared to the reference sample, the shrinkages of samples with CSA-CaO EA are reduced slightly at 24h. However, shrinkage is gradually decreased in the following 24 hours due to the shrinkage compensation from the formation of expansive hydration products from CSA-CaO EA. After that, the UHPCs

containing CSA-CaO EA shows slight increase in the autogenous shrinkage. At the age of 7d, the autogenous shrinkage of UH4 is reduced by 59% compared to that of the reference sample. As a result, the CSA-CaO EA is effective in reducing the autogenous shrinkage, and the main reduction period mainly locates during the first 48 hours. As the ettringite formation needs about 5-7 days to completely development its potential expansion, the CaO seems to be the decisive factor in influencing the shrinkage. Although the reduction of early-age shrinkage (before 24h) is limited, the CSA-Ca) EA can effectively compensate shrinkage at the age of 7 days, which may reduce the cracking risk of UHPC. However, no real expansion of UHPC samples was observed even 15% CSA-CaO EA is incorporated, this is different from the case of CSA-CaO EA in conventional concrete [3].

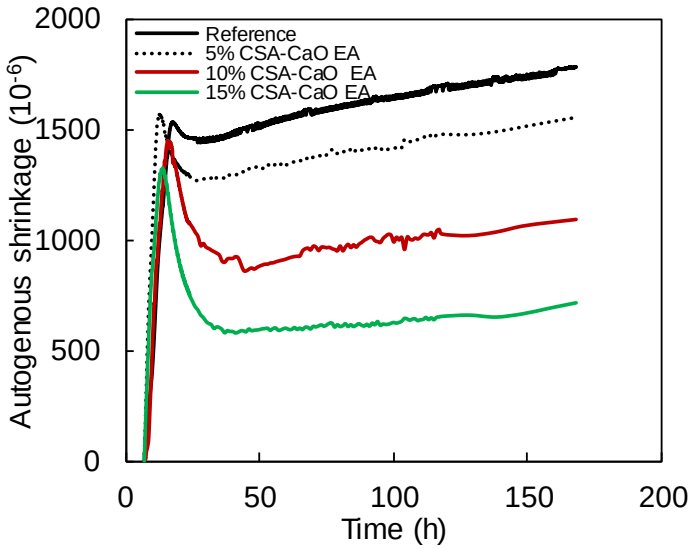

Figure 3 Influence of CSA-CaO EA on the autogenous shrinkage development of UHPC

3.3 Effect of CSA-CaO EA on hydration of UHPC

Figure 4 presents the heat flow and cumulative heat of UHPC pastes with 10% CSA-CaO EA and without CSA-CaO EA. The heat flow and cumulative heat curves are plotted up to 72h. It can be observed from Figure 4(a) that a dormant period of 6h is followed by an acceleration period and a main peak that manifests between 6h and 40h. After adding CSA-CaO EA, the heat flow of dormant period of cement hydration enhanced, and the heat flow of specimen with CSA-CaO EA is still higher than the reference sample until 10h. Also, the main peak of the heat flow is lower from 18h to 22h, indicating a delay effect on the hydration at the early age. This retardation effect of CSA-CaO EA on hydration is mainly present during the first day, after which the hydration flow

and cumulative heat are both higher than those of the reference sample. At the age of 3d, the cumulative heat of UHPC paste containing 10% CSA-CaO EA is increased by 19.5% compared to the reference sample. However, similar cumulative hydration heat is observed before 20h for these two samples, indicating that the hydration of the CSA-CaO EA during the first 24h is slow, but hydrates faster in the flowing 48h. This explain that the limited effect of CSA-CaO EA on the autogenous shrinkage before 20h and a rapid reduction of shrinkage is observed between 24h and 48h.

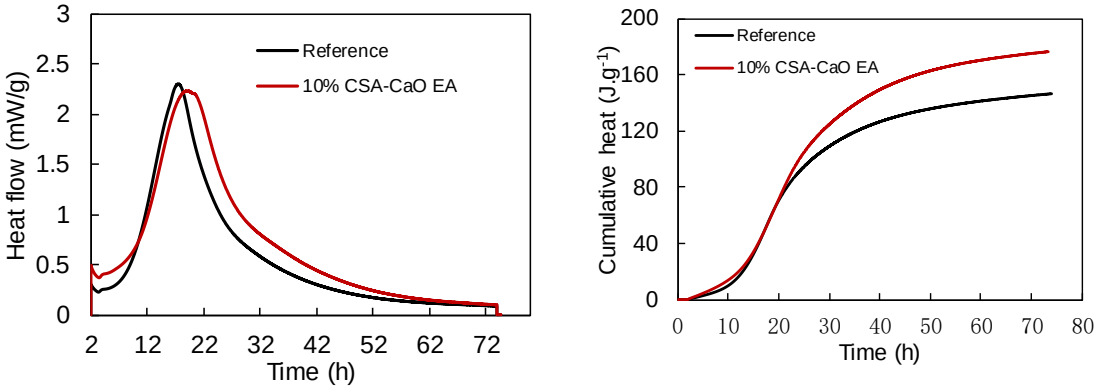

(a) heat flow (b) cumulative heat

Figure 4 Effect of CSA-CaO EA on the heat evolution of UHPC

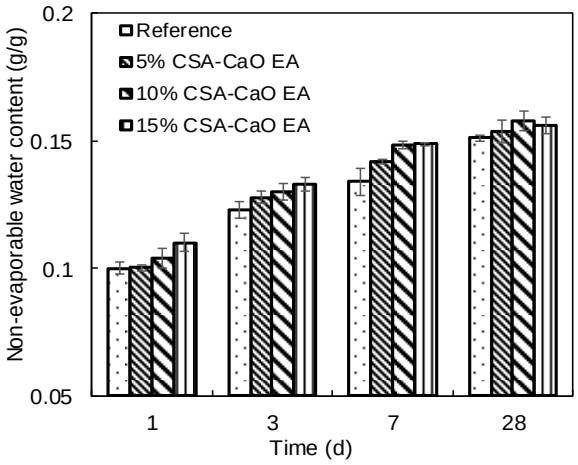

Figure 5 The non-evaporable water content of UHPC pastes at different ages

The non-evaporable water content of UHPC pastes containing different amounts of CSA-CaO EA are presented in Figure 5. It can be seen that the non-evaporable water content at the different ages is increased by adding CSA-CaO EA. Although the main peak of heat flow is delayed by adding CSA-CaO EA, the non-evaporable water contents of samples containing CSA-CaO EA at the age of 1d and 3d are improved, indicating the increasing hydration degree. This enhancement of hydration degree contributes to the improvement of mechanical properties at the early age (shown

in Figure 2). The higher non-evaporable water content means less free water in capillary pores, which may contribute to the reduction of RH.

3.4 The relative humidity characteristics of UHPC

Figure 6 shows the effect of CSA-CaO EA additions and w/b ratio on the internal RH of UHPC. It can be observed from Figure 6 (a) that all the samples show relatively low internal RH. The highest internal RH of reference UHPC is about 97.4% before setting, which is different from the internal RH of normal concrete (nearly 100% at the early hours) [42]. The measured internal RH is not only affected by the meniscus formation inducing capillary pressure, but also by the ion concentration in the pore solution [43]. Usually, this initial RH drop before setting is mainly attributed to dissolved salts in the pore fluid [44], but the unsaturated capillary pores also contribute to this RH drop, due to the lower RH of UHPC than that of high performance concrete (shown in Figure 6 (b)) [18]. When the CSA-CaO EA is added, the internal RH is reduced. In other words, more water participates in the hydration of cementitious materials compared to the reference sample. It is possible that the CSA-CaO EA accelerates the hydration of UHPC, resulting in the decreasing internal RH and increasing self-desiccation[45]. However, the tested autogenous shrinkage is obviously decreased by adding CSA-CaO EA. This is mainly due to the shrinkage compensation from the expansive hydrates overwhelms the effect of increasing self-desiccation on the shrinkage. Therefore, the CSA-CaO EA in UHPC possesses two kinds of effects on the autogenous shrinkage behaviour. Firstly, the acceleration of hydration improves the self-desiccation, which has a potential to increase the autogenous shrinkage. Secondly, the expansive products produced by the hydration of CSA-CaO EA can lead to swell stress. Because the effect of swelling stress on shrinkage overwhelms that of the improvement of self-desiccation, the autogenous shrinkage of the UHPC with CSA-CaO EA exhibits a reduction trend.

It can be observed from Figure 6 (b) that the development of the internal RH is closely related to the w/b ratio. The internal RH of concrete with high w/b reaches 99.8% at 6h, and then decrease gradually in the following curing age. However, the internal RH of UHPC containing different amount of CSA-CaO EA is low and rapidly reduces to 93% at 24h. As a result, lack of enough water for the reaction of CSA-CaO EA at the early age. Consequently, the shrinkage compensation and expansion of CSA-CaO EA in UHPC is limited.

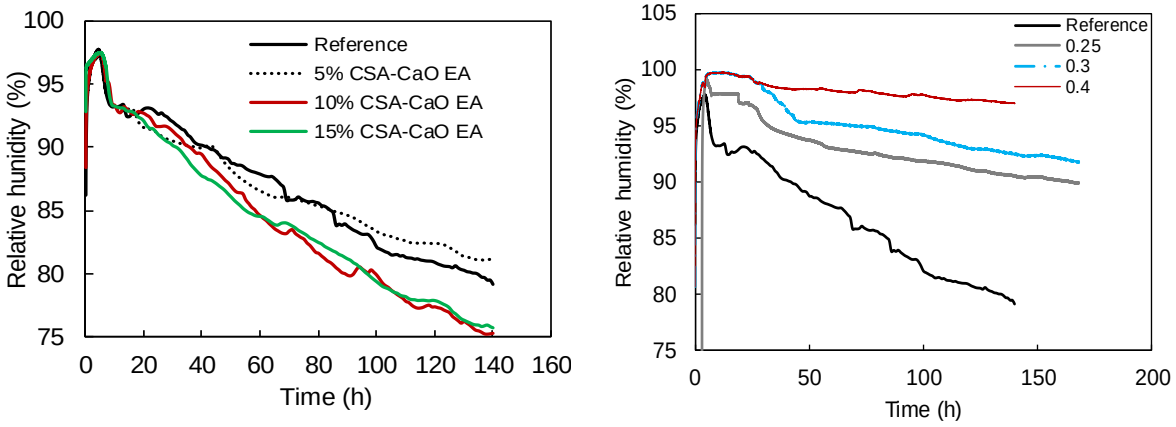

(a) the effect of CSA-CaO EA (b) the effect of w/b ratio

Figure 6 The effect of the CSA-CaO EA additions and w/b ratio on the internal RH of UHPC

3.5 Microstructure and hydration products

3.5.1 The XRD analysis

Figure 7 shows the XRD patterns of UHPC pastes containing different fractions of CSA-CaO EA. It can be observed that the main crystalline hydration products are ettringite, $Ca(OH)_2$ and monosulfoaluminate etc.. The presence of $Ca(OH)_2$ can be indicated by peaks at about $2\theta=17.9°$, $2\theta=28.6°$ and $2\theta=50.8°$ etc., and the content of $Ca(OH)_2$ can be qualitatively analyzed by the intensity of these peaks. As shown in Figure 7, the intensity of $Ca(OH)_2$ peak increases with the increasing CSA-CaO EA addition. In addition, large amounts of un-hydrated C_3S and C_2S are found due to the low w/b ratio, and their contents are probably increased by increasing CSA-CaO EA content. Furthermore, it should be noted that the intensity of the peak of ettringite is also enhanced after adding CSA-CaO EA. But the increment is not apparent and lower than that of expectation. This may be attributed to the transformation from ettringite to monosulfoaluminate and low water to cement ratio[2]. In this system, there are two kinds of expansive hydration products (ettringite and $Ca(OH)_2$) being produced from the CSA-CaO EA hydration. The results of Rietveld refinement show that the content of ettringite phase of UHPC paste with 0%, 5%, 10% and 15% CSA-CaO EA are 4.05 wt%, 6.74 wt%, 7.25 wt% and 7.46 wt%, respectively. The content of $Ca(OH)_2$ phase of UHPC paste with 0%, 5%, 10% and 15% CSA-CaO EA are 4.43 wt%, 5.91 wt%, 6.89 wt% and 8.51 wt%, respectively. These results indicate that the ettringite and $Ca(OH)_2$ both increase with the increasing content of CSA-CaO EA. The swelling stress from these two products will compensate the development of autogenous shrinkage. Meanwhile, the formation of ettringite can attract a large

number of water molecules which causes antiparticle repulsion[32]. Whereas the formation of $Ca(OH)_2$ consumes less water than that of ettringite. The tests in section 3.2 to section 3.5 show that the internal RH is low, and there is not enough water for the CSA-CaO EA hydration. In addition, although the content of CaO in CSA-CaO EA is much lower than CSA, more extra $Ca(OH)_2$ is produced than that of ettringite phase. Therefore, it is likely that the expansion from $Ca(OH)_2$ may be easy in UHPC with low w/b ratio, thus causing better overall expansion than that of pure calcium sulphoaluminate[46].

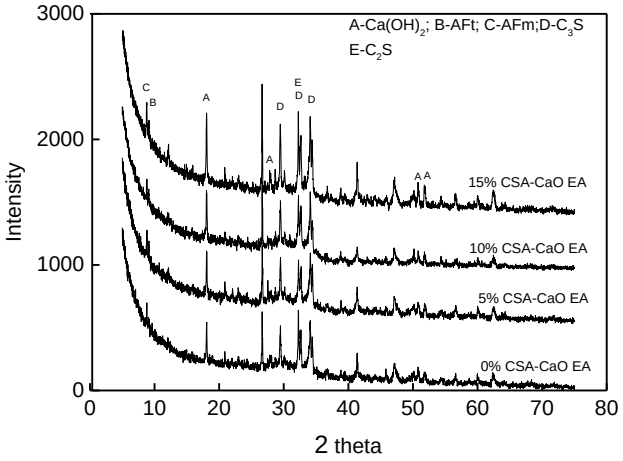

Figure 7 The XRD patterns of UHPC paste with different content of CSA-CaO EA

3.5.2 Thermal analysis

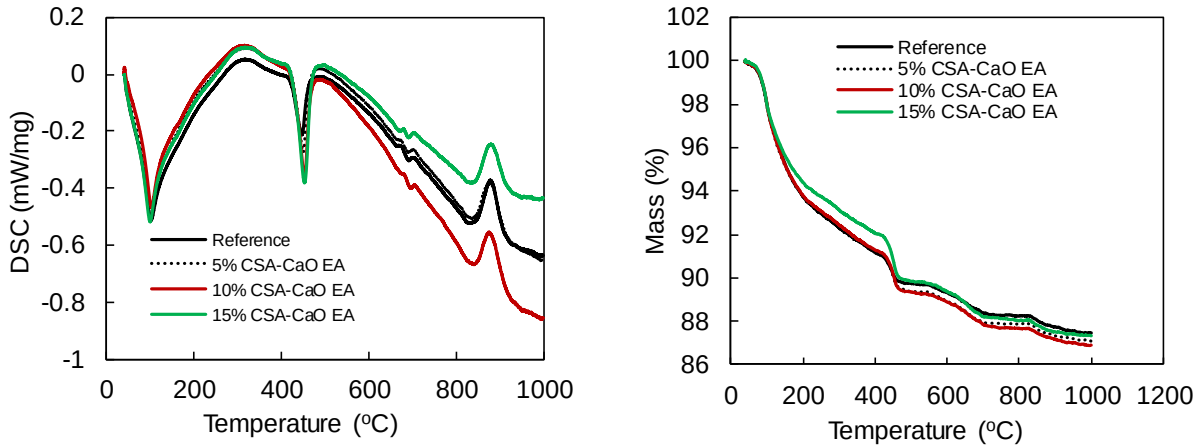

(a) DSC curve (b) TG curve

Figure 8 Thermal analysis curve of UHPC with different contents of CSA-CaO EA

Figure 8 shows the DSC and TG curves of UHPC pastes with different contents of CSA-CaO EA. It can be seen that all the samples exhibit high mass loss between 70°C and 300°C, which are mainly attributed to the dehydration of physically-bound water and hydration products (such as C-S-H gels, ettringite and monosulfoaluminate)[47, 48]. Figure 8(b) shows that the mass loss

between 70℃ and 300℃ of UHPC with 15% CSA-CaO EA is less than those of other samples. In addition, the total mass loss is increased by adding CSA-CaO EA due to the increasing mass loss between 400℃ and 500℃, but the total mass loss of UHPC with 15% CSA-CaO EA is still less than that of UHPC containing 5% and 10% CSA-CaO EA. It should be noted that the excessive amount of CSA-CaO EA reduces the mass loss between 200℃ and 400℃ due to its influence on the hydration and formation of C-S-H. Additionally, the mass loss between 410-510℃ indicates the decomposition of $Ca(OH)_2$ [49, 50]. The content of $Ca(OH)_2$ in hydrated cement paste can be calculated by the water loss. The calculated contents of $Ca(OH)_2$ are 5.61 % and 9.11 %, corresponding to the reference sample and sample containing 15% CSA-CaO EA, which means that 3.5% $Ca(OH)_2$ in the UHPC is additionally produced after the replacement of 15% CSA-CaO EA. A little mass loss between 660^{o}C and 720^{o}C is also observed in all the UHPC, representing the decomposition of calcium carbonate[51]. In general, it is clear that the amount of $Ca(OH)_2$ increases after the addition of CSA-CaO EA as well as the amount of the ettringite. As the main components of CSA-CaO EA are CaO and calcium sulphoaluminate. The chemical reactions of these crystals are as follows:

$$CaO + H_2O \rightarrow Ca(OH)_2 + \text{Heat (163.5kJ)} \quad (1)$$

$$C_4A_3S + H_2O \rightarrow \text{ettringite} \quad (2)$$

Figure 9 shows the TG and DTG curves of UHPC paste containing 10% CSA-CaO EA at 1d, 3d, 7d and 28d. It can be observed that the mass loss between 410^{o}C and 510^{o}C changes slightly with the curing age. It should be noted that the mass losses resulting from $Ca(OH)_2$ are 1.90% and 1.98% corresponding to the specimens at 1d and 3d, respectively. Moreover, the 7d and 28d-mass losses of specimens are 1.94% and 1.90% respectively. Hence, it can be concluded that the hydration of CaO mainly occurs during the first 3 days. The early formation of additional $Ca(OH)_2$ from the hydration of CSA-CaO EA is beneficial to the reduction of shrinkage during the first 24h. As the hydration proceeds, the $Ca(OH)_2$ content in cement-silica fume system will gradually decrease with the curing age[52] due to the continuous pozzolanic reaction. Usually, the pozzolanic reaction of silica fume mainly occurs after 3 days of hydration[53]. Therefore, the autogenous shrinkage of UHPC containing CSA-CaO EA also shows a slightly increasing trend after 3d as more hydration products were formed.

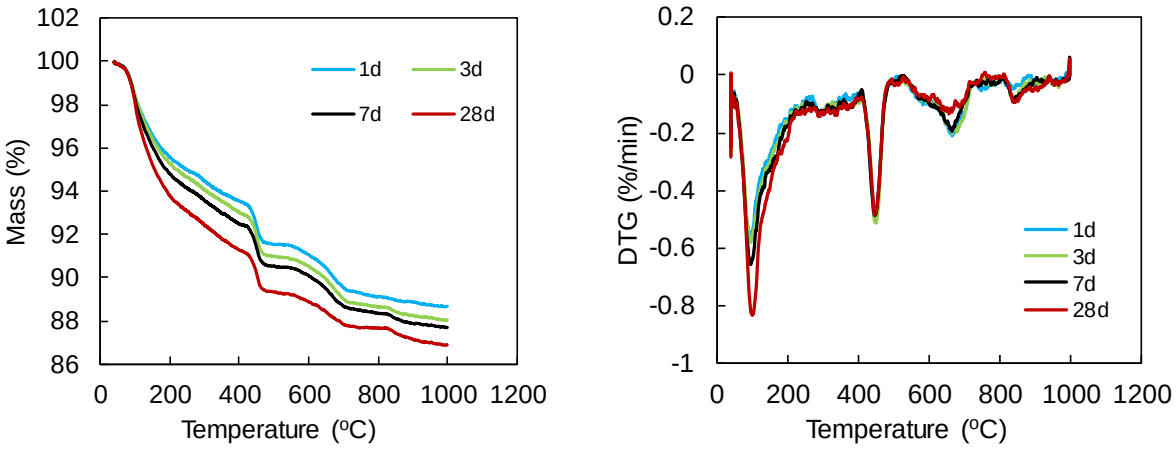

(a) TG curve (b) DTG curve

Figure 9 TG and DTG curves of UHPC paste containing 10% CSA-CaO EA at 1, 3, 7 and 28d

3.5.3 Scanning electron microscopy

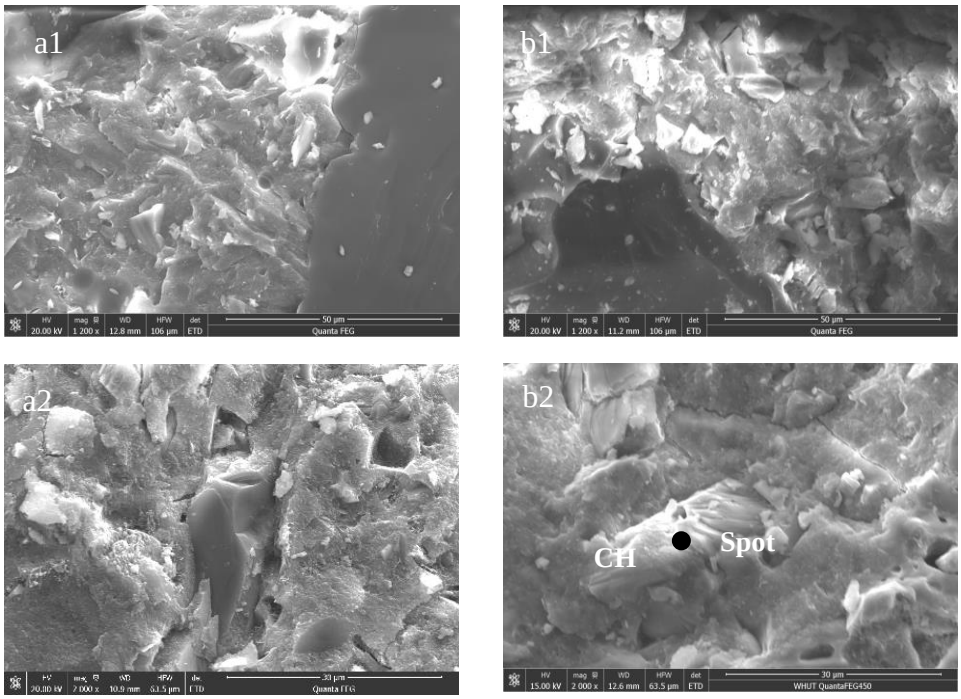

(a) without CSA-CaO EA (b) with 10% CSA-CaO EA

Figure 10 The morphology of UHPC specimens with and without CSA-CaO EA at 28d

Figure 10 shows the morphology of UHPC with and without CSA-CaO EA. It can be seen that there is no visible interfacial transition zone between the matrix and the aggregate, which is attributed to the high silica fume content, low w/b ratio and small size of aggregate [54], because the wall effect and the formation of $Ca(OH)_2$ is hindered in UHPC[55, 56]. In addition, there are some $Ca(OH)_2$ crystals with large grain sizes can be observed. The SEM-EDS analysis was used to clarify these crystals. The test result is shown in Figure 11. It can be observed that the O and Ca are the main chemicals in this area. The Ca/O ratio of the hydrates is about 0.46, which is very close to

the Ca/O ratio of $Ca(OH)_2$. This clarifies that this large crystal is $Ca(OH)_2$. Expansive products like $Ca(OH)_2$ disperse in the matrix, which promotes the reduction of the autogenous shrinkage. But it is difficult to find needle-like ettringite crystals, which may be wrapped the dense microstructure.

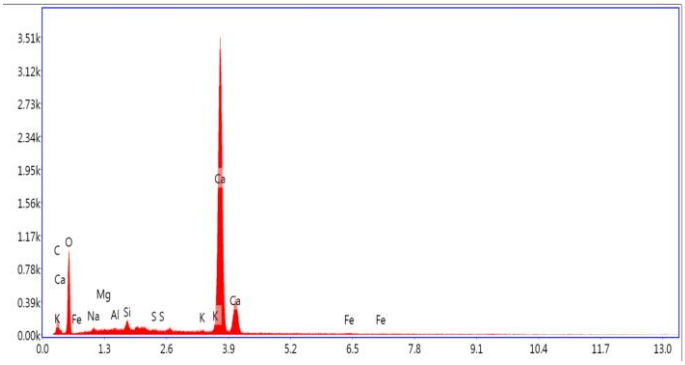

Figure 11 The SEM-EDS analysis of the spot in Figure 10

3.5.4 Pore structure

The pore structure curves of the UHPC are shown in Figure 12. The total porosities of UHPC with 0% and 10% CSA-CaO EA are similar. However, the pore size distribution is shifted to the left by adding 10% CSA-CaO EA. The volume of fine pores between 5nm and 50nm is significantly reduced, whereas the volume of pores larger than 100nm increases obviously for samples containing CSA-CaO EA. The increased volume of coarse pores may have an adverse effect on the permeability and mechanical properties. However, the reduction of the volume of fine pores between 5nm and 50nm would be beneficial to the reduction of the autogenous shrinkage. As the development of autogenous shrinkage is mainly related to the pores with size between 5nm and 50nm [57]. Therefore, the CSA-CaO EA shows an adverse effect on the pore size distribution of UHPC, and increases the average pore diameter [22], which is closely related to the development of the strength and the autogenous shrinkage.

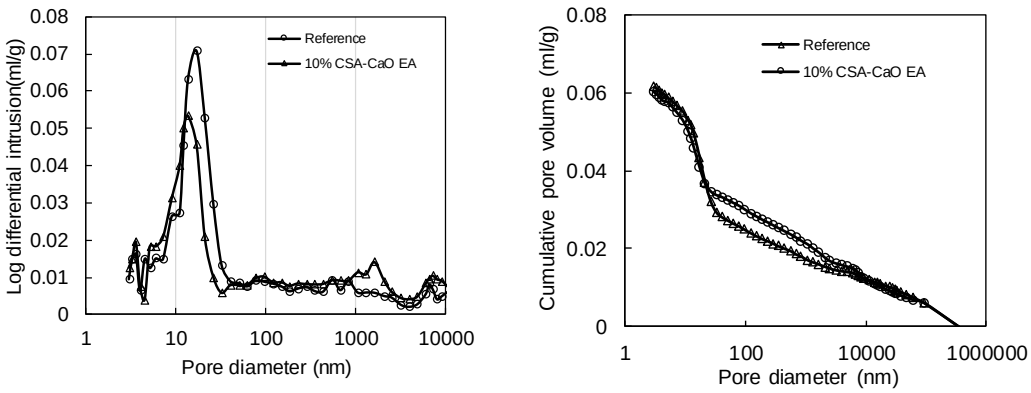

(a) Log differential intrusion (b) Cumulative pore volume

Figure 12 The pore structure of UHPC containing different amount of CSA-CaO EA

4 Discussions

4.1 Expansion mechanism of CSA-CaO EA in UHPC

According to the previous studies[33, 58-60], expansive concrete or high performance concrete can be prepared by using different kinds of CSA-CaO EA. However, it cannot compensate the shrinkage of UHPC completely by using CSA-CaO EA. Based on the test results above, there are some reasons or mechanisms limiting the expansion property of the CSA-CaO EA in UHPC.

(1) Rapid decrease of internal RH and significant high early autogenous shrinkage

After setting, as the pores in UHPC are unsturated, a large number of partially-filled pores are created in the matrix. The pore solution menisci exsisting in these pores induces capillary pressure, producing self-desiccation[61]. The capillary pressure obtained from self-desiccation will produce measurable shrinkage. According to Kelvin equation, as the self-desiccation occurs and capillary pressure increases, there will be a concurrent reduction in the internal RH [62-64]. The relationship between RH and the size of pores being empty can be established according to the Young's equation and Kelvin equation [65] (shown in Figure 13). Based on the RH development of UHPC, it can be observed from Figure 13 that the pores larger than 62nm is emptying at 6h, indicating that numerous capillary pores in the matrix are not saturated at the early age. As the internal RH decreases rapidly, the pores larger than 17nm is emptying at 24h, leading to a significantly high autogenous stresses and strains. Because the modulus of elasticity and mechanical strength are still very low, the volume of UHPC performs is easily deformed. Therefore, a large autogenous shrinkage can be observed at the early age (such as 24h). However, the hydration of the CSA-CaO EA is hindered due to the rapid decreasing of internal RH, which makes the expansion from CSA-CaO EA is not sufficient for compensating the shrinkage of UHPC.

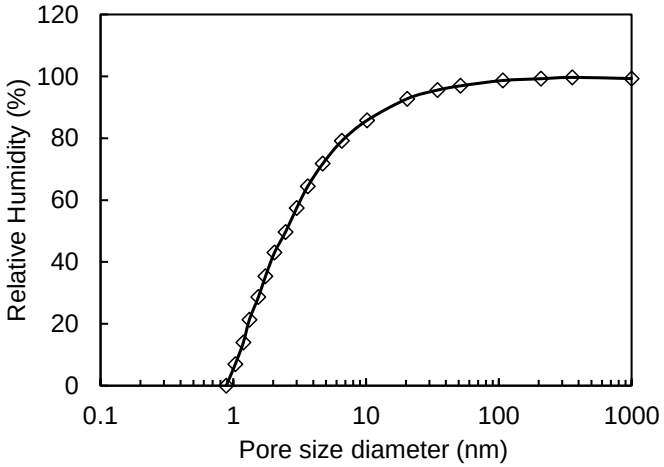

Figure 13 Relationship between relative humidity and size of emptying pores according to the Young's equation and Kelvin equation [65]

(2) Compact microstructure

A paste specimen with water to cement ratio of 0.4 was prepared for MIP test. The pore structures of UHPC paste and normal cement paste are shown in Figure 14. The test results show that although the porosity of UHPC is much lower than that of normal concrete, the volume of pores with the diameter between 5nm and 50nm of UHPC is much higher than that of the normal cement paste. Because the pores between 5nm and 50nm is closely related to the autogenous shrinkage[57], this refinement acturally increases the autogenous shrinkage.

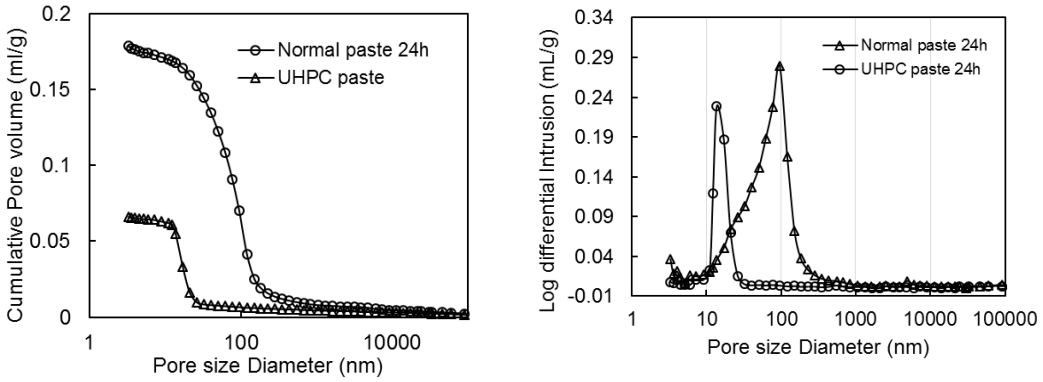

(a) Cumulative pore volume (b) Log differential intrusion

Figure 14 The pore size distribution of UHPC and normal concrete

It can be indicated from the porosity of the UHPC at 24h that the UHPC has dense compacted matrix at early age. Fillers (silica fume and fly ash in this study) are used in UHPC, which leads to an optimum packing of the granular ingredients of UHPC, and further contributes to the mechancial properties and durability[66]. The diagrams that describe the microstructure of two pastes are proposed and shown in Figure 15. As is shown in Figure 15 (a), the slip gaps of framework between

large particles (mainly cement) are filled by silica fume, which reduces the amount of water that fills in the void of the blending materials[67]. Meanwhile, the low w/b ratio together with the filling effect allow the UHPC to have a high packing density of the fine powders, resulting in a compact microstructure and low porosity [68]. However, for normal concrete, the particles suspend in the water[69]. The Figure 15 (b) describe the microstructure of normal concrete paste. The pores around the CSA-CaO EA particles are large and the water can contact the CSA-CaO EA thoroughly. But for CSA-CaO EA in UHPC, there are limited voids for the expansive hydration products. Also the silica fume surrounds the CSA-CaO EA, which forms a dense zone that has low porosity [70]. This dense zone not only prevents the CSA-CaO EA from contacting water directly but also the water from transporting from the fine empty pores to the CSA-CaO EA. Therefore, the hydration of CSA-CaO EA and development of expansive products in UHPC are hindered.

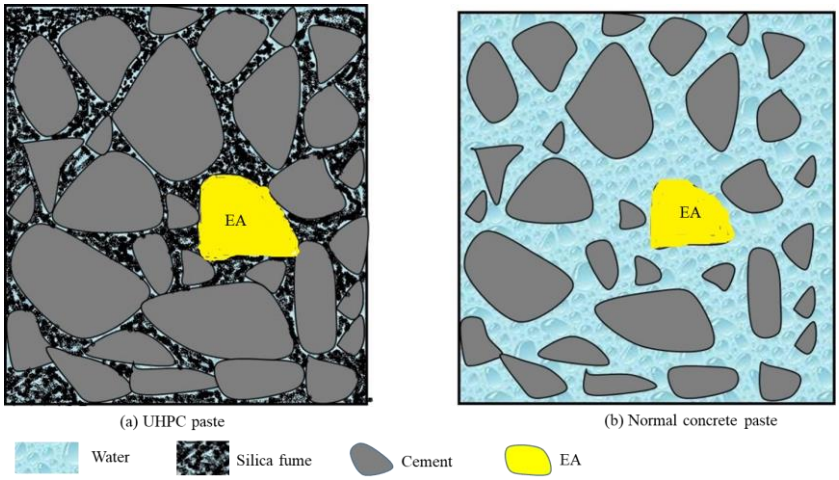

Figure 15 The schematic diagram of microstructure of UHPC and normal concrete at the early age

(3) The potential exchange of water between solids

In case of the UHPC paste, the CSA-CaO EA particles are surrounded by fine silica fume (shown in Figure 15). Likely the interface between aggregate and cement paste[71], there may be interfacial zone with higher porosity than that of silica fume paste. A previous study showed that the water in coarse pores would be released easily at high internal RH[72]. When the internal RH decreased, the water would move from coarser pores to finer pores[73, 74]. The free water around the CSA-CaO EA will move from the interfacial zone to fine pores in silica fume paste when it is still mixture. As the hydration proceeds, the compact hydrates are formed near the cement particles, which can be called inner product. The hydration products (outer product) around the CSA-CaO EA

are produced earlier than the inner product, but they shows a looser microstructure[75]. According to the water movement rule, it is likely that the water will move from outer product zone to the inner product zone. This water movement between solids may further hinders the hydration and its expansion of the CSA-CaO EA in UHPC.

(4) Out-sync of the time "window" of expansion and time "window" of shrinkage

The rapid decrease of RH during the first 24h leads to the significant high autogenous shrinkage. The main reduction of autogenous can be observed between 24h and 72h, but the high strength makes the volume deformation difficult. The effect of CSA-CaO EA on the shrinkage is weakened by the time inconsistency of expansion and shrinkage. In other words, the time "window" of expansion does not synchronize with the time "window" of shrinkage. Meanwhile, the rapid reduction of internal RH at the early age hinders the hydration of CSA-CaO EA. Therefore, the time differences between expansion "window" of the CSA-CaO EA and the shrinkage "window" play an important role in hindering the expansion effect of CSA-CaO EA in UHPC.

4.2 Strategies on improving the expansion property of EA

Based on the studies on the expansion mechanisms of CSA-CaO EA in UHPC, some strategies are proposed to further reduce the autogenous shrinkage of UHPC by adding EA. The suggestions are as following:

(1) Uniform the time "window" of expansion of EA and time "window" of shrinkage of UHPC

Relations between the development of autogenous shrinkage and expansion from EA are important for the reduction of shrinkage. The test results show that a large shrinkage value of 1200με can be found at 24h. If the occurrence of main expansion from the hydration of EA is later than that of shrinkage, the expansion effect will be weakened due to the increase of the dense microstructure and the mechanical strength. Therefore, in order to reduce the autogenous shrinkage by adding EA, the time "window" of expansion and time "window" of shrinkage should be uniformed. As shown in Figure 16, the expansion should be mainly produced at the same time when the autogenous shrinkage develops rapidly. In case of the EA in UHPC, the time "window" of expansion should be moved forward, and most of the expansion of EA should be achieved before 24h corresponding to the development of shrinkage. As the reaction of CaO mainly occurs within

1-2days, the addition of CaO would be more effective in compensating shrinkage than CSA. The higher portion of CaO in combined EA, the larger reduction of shrinkage will be found within 2 days. Therefore, it is better to choose a type of EA with high proportion of CaO and high reactivity.

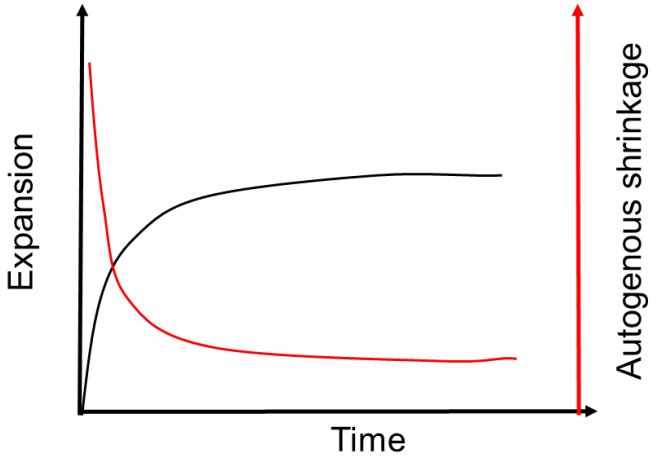

Figure 16 Relationship between the expansion and autogenous shrinkage of UHPC

（2）Using EA with high reactivity and low water consumption

The low RH of UHPC hinders the hydration of cementitious materials as well as EA. If the reactivity of EA is low, there will be little water left when it starts to hydrate. In that event, less shrinkage compensation will be achieved. In addition, if the EA hydration needs to consume large amount of water (such as ettringite based EA), the low water content in UHPC would makes it difficult to hydrate. Therefore, the EA with high reactivity and low water consumption will be suitable for the shrinkage reduction.

4.3 Experimental validations

Experiments were conducted to confirm whether the proposed suggestions are helpful to reduce the autogenous shrinkage of UHPC by adding EA. According a previous study, the CaO based EA with little water consumption[76] possesses excellent ability to compensate shrinkage of high performance concrete[35]. Therefore, a kind of high reactive CaO based EA is also used. In order to improve the reactivity of EA, it is ground into a high Blaine fineness (>600m^2/kg) firstly. Effects of the CaO based EA on autogenous shrinkage and hydration evolution of UHPC are shown in Figure 17 and Figure 18, respectively. It can be observed that the autogenous shrinkage is significantly reduced by adding high reactive CaO based EA. Even a slight expansive behaviour can be observed in the UHPC containing 10% CaO based EA. It should be noted that the CaO based EA not only reduces shrinkage within 24h, but also compensates shrinkage until 7d. The latter may be

attributed to expansion from little amount of ettringite and delayed hydration of CaO due to rapid decreasing RH.

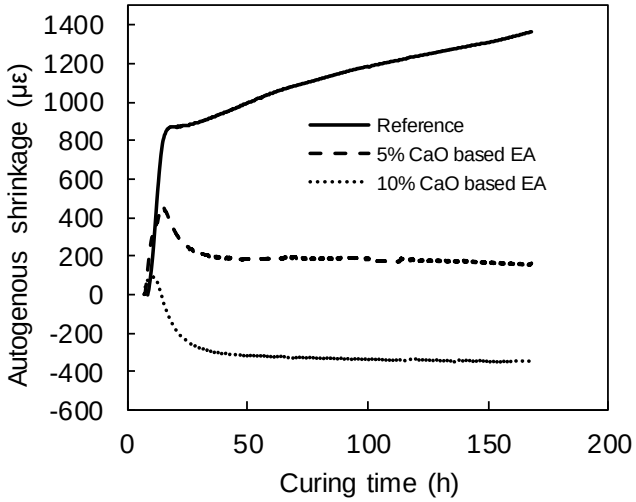

Figure 17 Effect of CaO based EA on the autogenous shrinkage of UHPC

In Figure 18, the early hydration of UHPC paste is obviously accelerated by adding CaO based EA. Before 24h, the heat flow is much higher than that of the reference sample. This means that the CaO based EA hydrates rapidly within 24h, which corresponds to the development period of autogenous shrinkage. Therefore, the time "window" of expansion and time "window" of shrinkage are synchronized by using high reactive CaO based EA. As a result, the swelling stress from formation of expansive $Ca(OH)_2$ compensates the autogenous shrinkage. By using this high reactive EA, a low shrinkage or slight expansive UHPC can be prepared. From the experiment results, it can be concluded that low shrinkage or expansive UHPC is possible to prepare by synchronizing the hydration of CaO based EA with autogenous shrinkage development/internal RH. For the expansive UHPC, further research on the expansion mechanism of CaO based EA will be studied in the future.

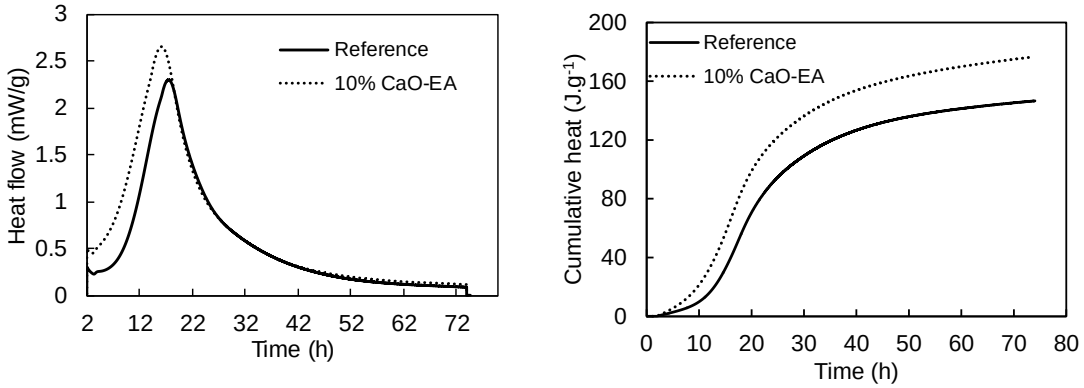

(a) Heat flow (b) Cumulative heat

Figure 18 Effect of CaO based EA on the heat flow and cumulative heat of UHPC

5 Conclusions

This study presents the effect of CSA-CaO EA on the volume stability, mechanical properties, microstructure and hydration products of UHPC. The expansion mechanism of the CSA-CaO EA in UHPC is systematically explored. Strategies and experimental validation on improving the shrinkage compensation of EA are discussed. Based on the findings, the following conclusions can be drawn.

(1) Compared to the reference UHPC, the autogenous shrinkage is obviously reduced by adding the CSA-CaO based EA. The reduction of shrinkage mainly occurs between 24h and 48h. Also, the mechanical properties are improved by adding CSA-CaO EA at the early age, but an adverse effect on mechanical properties is observed at 7d and 28d with the addition of CSA-CaO EA.

(2) The heat flow of the dormant period of cement hydration is accelerated, but the main peak of heat flow is delayed by adding CSA-CaO EA. The hydration is accelerated by CSA-CaO EA between 20h and 72h, resulting in a higher hydration degree of the UHPC than that of the reference sample. The additional $Ca(OH)_2$ and ettringite are produced by the hydration of CSA-CaO EA, which causes an overall reduction of autogenous shrinkage at the early age.

(3) The internal RH of UHPC is relatively low (97.4%) before setting, and is rapidly reduced to about 93% at 24h, leading to a significant high autogenous stresses and strains. Therefore, a large autogenous shrinkage can be found at early age. The addition of CSA-CaO EA further reduces the RH and increases the self-desiccation. When the CSA-CaO EA is present, the volume of pores with a size of between 5nm and 50nm is significantly reduced, which contributes to the increase of shrinkage and mechanical properties.

(4) The addition CSA-CaO EA can mitigate the shrinkage of UHPC, but the efficiency is still not very high. The reasons related to the limited expansion property of CSA-CaO EA in UHPC are explored as follows. a) Rapid decrease of internal RH and significantly high early-age autogenous shrinkage results in insufficient expansion from CSA-CaO EA for shrinkage compensation; b) The compact microstructure and the surroundings of silica fume hinder the hydration of the CSA-CaO EA; c) The water tends to move away from the CSA-CaO EA to the silica fume paste and the inner hydration products; d) The effect of CSA-CaO EA is weakened by the out-sync of the time “window” of expansion and time “window” of shrinkage.

(5) Based on the expansion mechanisms and the experimental validations of CSA-CaO EA in

UHPC, the high reactive CaO based EA with low water consumption that can synchronize the time "window" of expansion and time "window" of shrinkage and can be effective in reducing the autogenous shrinkage of UHPC.

Acknowledgements

This work was financially supported by the National Key R&D Program of China (No. 2017YFB0310001).

References

[1] F. de Larrard, T. Sedran, Optimization of ultra-high-performance concrete by the use of a packing model, Cement and Concrete Research 24(6) (1994) 997-1009.

[2] M. Cheyrezy, V. Maret, L. Frouin, Microstructural analysis of RPC (Reactive Powder Concrete), Cement and Concrete Research 25(7) (1995) 1491-1500.

[3] D.Y. Yoo, S.W. Kim, Y.S. Yoon, J.J. Park, Benefits of using expansive and shrinkage-reducing agents in UHPC for volume stability, Magazine of Concrete Research 66(14) (2015) 745-750.

[4] D.Y. Yoo, J.J. Park, S.W. Kim, Y.S. Yoon, Early age setting, shrinkage and tensile characteristics of ultra high performance fiber reinforced concrete, Construction & Building Materials 41(41) (2013) 427-438.

[5] A.M. Paillere, M. Buil, J. Serrano, Effect of fiber addition on the autogenous shrinkage of silica fume, ACI Materials Journal 86(2) (1989).

[6] P. Lura, O.M. Jensen, J. Weiss, Cracking in cement paste induced by autogenous shrinkage, Materials and structures 42(8) (2009) 1089-1099.

[7] J. Brooks, J. Cabrera, M.M. Johari, 11 FACTORS AFFECTING THE AUTOGENOUS SHRINKAGE OF SILICA FUME HIGH-STRENGTH CONCRETE, Autogenous shrinkage of concrete: proceedings of the international workshop, organised by JCI (Japan Concrete Institute), Hiroshima, June 13-14, 1998, Taylor & Francis, (1999), 195.

[8] Y. Yang, R. Sato, K. Kawai, Autogenous shrinkage of high-strength concrete containing silica fume under drying at early ages, Cement and Concrete Research 35(3) (2005) 449-456.

[9] A.K. Cheung, C.K. Leung, Shrinkage reduction of high strength fiber reinforced cementitious composites (HSFRCC) with various water-to-binder ratios, Cement and Concrete Composites 33(6) (2011) 661-667.

[10] O.M. Jensen, P.F. Hansen, Autogenous deformation and RH-change in perspective, Cement and Concrete Research 31(12) (2001) 1859-1865.

[11] D.P. Bentz, O.M. Jensen, Mitigation strategies for autogenous shrinkage cracking, Cement and Concrete Composites 26(6) (2004) 677-685.

[12] E.-i. Tazawa, S. Miyazawa, Influence of cement and admixture on autogenous shrinkage of cement paste, Cement and concrete research 25(2) (1995) 281-287.

[13] P. Lura, M. Wyrzykowski, C. Tang, E. Lehmann, Internal curing with lightweight aggregate

produced from biomass-derived waste, Cement & Concrete Research 59(59) (2014) 24-33.
[14] L.L. Peiliang Shen , Fazhou Wang, Yongjia He, Shuguang Hu, Internal curing using lightweight fine aggregate in ultra-high performance concrete, Cement & Concrete Composites (2019) (submitted).
[15] V. Mechtcherine, Use of superabsorbent polymers (SAP) as concrete additive, RILEM Technical Letters 1 (2016) 81-87.
[16] F. Wang, J. Yang, S. Hu, X. Li, H. Cheng, Influence of superabsorbent polymers on the surrounding cement paste, Cement and Concrete Research 81 (2016) 112-121.
[17] C. Schröfl, V. Mechtcherine, M. Gorges, Relation between the molecular structure and the efficiency of superabsorbent polymers (SAP) as concrete admixture to mitigate autogenous shrinkage, Cement and concrete research 42(6) (2012) 865-873.
[18] H. Huang, G. Ye, Examining the “time-zero” of autogenous shrinkage in high/ultra-high performance cement pastes, Cement & Concrete Research 97 (2017) 107-114.
[19] N.V. Tuan, G. Ye, K.V. Breugel, Internal curing of ultra high performance concrete by using rice husk ash, International Conference on Material Science and Rilem Week, Rilem, 2010.
[20] H.F.W. Taylor, Cement chemistry, 2nd ed., T. Telford, London, 1997.
[21] D.P. Bentz, O.M. Jensen, K.K. Hansen, J.F. Olesen, H. Stang, C.J. Haecker, Influence of Cement Particle-Size Distribution on Early Age Autogenous Strains and Stresses in Cement-Based Materials, Journal of the American Ceramic Society 84(1) (2001) 129-135.
[22] S. Nagataki, H. Gomi, Expansive admixtures (mainly ettringite), Cement & Concrete Composites 20(2–3) (1998) 163-170.
[23] T. Higuchi, M. Eguchi, M. Morioka, E. Sakai, Hydration and properties of expansive additive treated high temperature carbonation, Cement & Concrete Research 64(10) (2014) 11-16.
[24] W. Sun, H. Chen, X. Luo, H. Qian, The effect of hybrid fibers and expansive agent on the shrinkage and permeability of high-performance concrete, Cement and Concrete Research 31(4) (2001) 595-601.
[25] L. Mo, M. Deng, M. Tang, Effects of calcination condition on expansion property of MgO-type expansive agent used in cement-based materials, Cement & Concrete Research 40(3) (2010) 437-446.
[26] J.J. Park, D.Y. Yoo, S.W. Kim, Y.S. Yoon, Drying shrinkage cracking characteristics of ultra-high-performance fibre reinforced concrete with expansive and shrinkage reducing agents, Magazine of Concrete Research 65(4) (2013) 248-256.
[27] D.Y. Yoo, J.J. Park, S.W. Kim, Y.S. Yoon, Combined effect of expansive and shrinkage-reducing admixtures on the properties of ultra high performance fiber-reinforced concrete, Journal of Composite Materials 48(16) (2014) 1981-1991.
[28] C. Maltese, C. Pistolesi, A. Lolli, A. Bravo, T. Cerulli, D. Salvioni, Combined effect of expansive and shrinkage reducing admixtures to obtain stable and durable mortars, Cement & Concrete Research 35(12) (2005) 2244-2251.
[29] D.Y. Yoo, J.J. Park, S.W. Kim, Y.S. Yoon, Evaluating Early Age Shrinkage Behavior of Ultra High Performance Cementitious Composites (UHPCC) with CSA Expansive Admixture and Shrinkage Reducing Agent, Journal of the Korea Concrete Institute 23(4) (2011) 655-657.
[30] M. Gesoglu, E. Güneyisi, A.H. Nahhab, H. Yazıcı, Properties of ultra-high performance fiber reinforced cementitious composites made with gypsum-contaminated aggregates and cured at normal and elevated temperatures, Construction & Building Materials 93 (2015) 427-438.

[31] M. Valipour, K.H. Khayat, Coupled effect of shrinkage-mitigating admixtures and saturated lightweight sand on shrinkage of UHPC for overlay applications, Construction and Building Materials 184 (2018) 320-329.
[32] P.K. Mehta, Mechanism of expansion associated with ettringite formation, Cement and Concrete Research 3(1) (1973) 1-6.
[33] M. Wyrzykowski, G. Terrasi, P. Lura, Expansive high-performance concrete for chemical-prestress applications, Cement & Concrete Research 107 (2018) 275-283.
[34] P. Shen, L. Lu, Y. He, F. Wang, S. Hu, Hydration of quaternary phase-gypsum system, Construction & Building Materials 152 (2017) 145-153.
[35] V. Corinaldesi, A. Nardinocchi, J. Donnini, The influence of expansive agent on the performance of fibre reinforced cement-based composites, Construction and Building Materials 91 (2015) 171-179.
[36] M.J. Oliveira, A.B. Ribeiro, F.G. Branco, Combined effect of expansive and shrinkage reducing admixtures to control autogenous shrinkage in self-compacting concrete, Construction and Building Materials 52 (2014) 267-275.
[37] Expansive agents for concrete, China Standard Press, 2009.
[38] M.S. Meddah, M. Suzuki, R. Sato, Influence of a combination of expansive and shrinkage-reducing admixture on autogenous deformation and self-stress of silica fume high-performance concrete, Construction and Building Materials 25(1) (2011) 239-250.
[39] H. Shuguang, L. Yue, Research on the hydration, hardening mechanism, and microstructure of high performance expansive concrete, Cement and concrete research 29(7) (1999) 1013-1017.
[40] W. Chen, H.J.H. Brouwers, Hydration of mineral shrinkage-compensating admixture for concrete: An experimental and numerical study, Construction & Building Materials 26(1) (2012) 670-676.
[41] D. Shen, X. Wang, D. Cheng, J. Zhang, G. Jiang, Effect of internal curing with super absorbent polymers on autogenous shrinkage of concrete at early age, Construction & Building Materials 106 (2016) 512-522.
[42] J.-K. Kim, C.-S. Lee, Moisture diffusion of concrete considering self-desiccation at early ages, Cement and Concrete Research 29(12) (1999) 1921-1927.
[43] P. Lura, O.M. Jensen, K. van Breugel, Autogenous shrinkage in high-performance cement paste: an evaluation of basic mechanisms, Cement and Concrete Research 33(2) (2003) 223-232.
[44] O.M. Jensen, Autogenous deformation and RH-change—self-desiccation and self-desiccation shrinkage, Building Materials Laboratory, The Technical University of Denmark, Lyngby, Denmark 285 (1993) 93.
[45] E.-i. Tazawa, Autogenous shrinkage of concrete, CRC Press1999.
[46] W. Chen, J. Qian, B. He, J. Liu, L. Zhang, X. Jia, Effects of Expansive Agent and Shale Pottery on Shrinkage Reduction of Lower Water-cement Ratio Mortar, Journal of the Chinese Ceramic Society 41(4) (2013) 505-510(6).
[47] F.M. Lea, The chemistry of cement and concrete, (1970).
[48] D.L. Kong, J.G. Sanjayan, Effect of elevated temperatures on geopolymer paste, mortar and concrete, Cement and concrete research 40(2) (2010) 334-339.
[49] Y. Fang, J. Chang, Microstructure changes of waste hydrated cement paste induced by accelerated carbonation, Construction and Building Materials 76 (2015) 360-365.
[50] J. Chang, Y. Li, M. Cao, Y. Fang, Influence of magnesium hydroxide content and fineness on the carbonation of calcium hydroxide, Construction and Building Materials 55 (2014) 82-88.

[51] S. Lim, P. Mondal, Effects of incorporating nanosilica on carbonation of cement paste, Journal of Materials Science 50(10) (2015) 3531-3540.
[52] C.-S. Poon, L. Lam, S. Kou, Y.-L. Wong, R. Wong, Rate of pozzolanic reaction of metakaolin in high-performance cement pastes, Cement and Concrete Research 31(9) (2001) 1301-1306.
[53] J. Zelić, D. Rušić, D. Veža, R. Krstulović, The role of silica fume in the kinetics and mechanisms during the early stage of cement hydration, Cement and Concrete Research 30(10) (2000) 1655-1662.
[54] A. Cwirzen, V. Penttala, C. Vornanen, Reactive powder based concretes: Mechanical properties, durability and hybrid use with OPC, Cement and Concrete Research 38(10) (2008) 1217-1226.
[55] A. Cwirzen, The effect of the heat-treatment regime on the properties of reactive powder concrete, Advances in Cement Research 19(1) (2007) 25-33.
[56] H. Zanni, M. Cheyrezy, V. Maret, S. Philippot, P. Nieto, Investigation of hydration and pozzolanic reaction in Reactive Powder Concrete (RPC) using 29Si NMR, Cement & Concrete Research 26(1) (1996) 93-100.
[57] P.K. Mehta, P.J.M. Monteiro, I. ebrary, Concrete: microstructure, properties, and materials, McGraw-Hill New York2006.
[58] W. Sun, H. Chen, X. Luo, H. Qian, The effect of hybrid fibers and expansive agent on the shrinkage and permeability of high-performance concrete, Cement & Concrete Research 31(4) (2001) 595-601.
[59] X.F. Wang, C. Fang, D.W. Li, N.X. Han, F. Xing, A self-healing cementitious composite with mineral admixtures and built-in carbonate, Cement & Concrete Composites (2018).
[60] S. Monosi, R. Troli, O. Favoni, F. Tittarelli, Effect of SRA on the expansive behaviour of mortars based on sulphoaluminate agent, Cement & Concrete Composites 33(4) (2011) 485-489.
[61] V.-T.-A. Van, C. Rößler, D.-D. Bui, H.-M. Ludwig, Rice husk ash as both pozzolanic admixture and internal curing agent in ultra-high performance concrete, Cement & Concrete Composites 53 (2014) 270-278.
[62] B. Persson, Self-desiccation and its importance in concrete technology, Materials & Structures 30(5) (1997) 293-305.
[63] S. Gaurav, D. Mukul, B. Dale, L. Pietro, C.F. Ferraris, J.W. Bullard, W. Jason, Detecting the Fluid-to-Solid Transition in Cement Pastes: Comparing experimental and numerical techniques, Concrete International (2009).
[64] S.B. L Barcelo, S Rigaud, P Acker, B Clavaud, Linear vs. volumetric autogenous shrinkage measurement: material behaviour or experimental artefact, proceedings of Self-dessiccation and its importance in concrete technology (1999) 109-125.
[65] D.P. Bentz, W.J. Weiss, Internal Curing: A 2010 State-of-the-Art Review, NIST Interagency/Internal Report (NISTIR) - 7765 (2011).
[66] H. Brouwers, H. Radix, Self-compacting concrete: theoretical and experimental study, Cement and Concrete Research 35(11) (2005) 2116-2136.
[67] Y. Qing, Z. Zenan, K. Deyu, C. Rongshen, Influence of nano-SiO2 addition on properties of hardened cement paste as compared with silica fume, Construction and building materials 21(3) (2007) 539-545.
[68] K. Droll, Influence of additions on ultra high performance concretes–grain size optimisation, Proceedings of the International Symposium on UHPC, Kassel, Germany, 2004, pp. 285-301.
[69] A.M. Neville, Properties of concrete, 4th and final ed., Wiley, New York, 1996.

[70] R. Yu, P. Spiesz, H.J.H. Brouwers, Mix design and properties assessment of Ultra-High Performance Fibre Reinforced Concrete (UHPFRC), Cement & Concrete Research 56 (2014) 29-39.
[71] G. Prokopski, J. Halbiniak, Interfacial transition zone in cementitious materials, Cement & Concrete Research 30(4) (2000) 579-583.
[72] J. Clarke, Lightweight Aggregate Concrete, Science, technology and Applications, Concrete (Feb) (2003).
[73] J. Castro, L. Keiser, M. Golias, J. Weiss, Absorption and desorption properties of fine lightweight aggregate for application to internally cured concrete mixtures, Cement & Concrete Composites 33(10) (2011) 1001-1008.
[74] D.P. Bentz, K.K. Hansen, H.D. Madsen, F. Vallée, E.J. Griesel, Drying/hydration in cement pastes during curing, Materials & Structures 34(9) (2001) 557-565.
[75] J.J. Chen, L. Sorelli, M. Vandamme, F.J. Ulm, G. Chanvillard, A Coupled nanoindentation/SEM-EDS study on low water/cement ratio Portland cement paste: evidence for C–S–H/Ca (OH) 2 nanocomposites, Journal of the American Ceramic Society 93(5) (2010) 1484-1493.
[76] M. Collepardi, R. Troli, M. Bressan, F. Liberatore, G. Sforza, Crack-free concrete for outside industrial floors in the absence of wet curing and contraction joints, Cement & Concrete Composites 30(10) (2008) 887-891.